Interferometric enhancement of x-ray reflectivity from unperturbed Langmuir monolayers of amphiphiles at the liquid-gas interface

Venkata Krishnan,[1] Joseph Strzalka,[1,2] Jing Liu,[1] Chian Liu,[2] Ivan Kuzmenko,[2] Thomas Gog,[2] and J. Kent Blasie[1,*]
[1]*Department of Chemistry, University of Pennsylvania, Philadelphia, Pennsylvania 19104, USA*
[2]*Advanced Photon Source, Argonne National Laboratory, Argonne, Illinois 60439, USA*
(Received 3 August 2009; revised manuscript received 24 November 2009; published 12 February 2010)

Langmuir monolayers provide an important system for the investigation of the intramolecular structure and intermolecular ordering of organic and bio-organic macromolecular amphiphiles at an interface between polar and nonpolar media, e.g., the liquid-gas interface. Specular x-ray and neutron reflectivity have contributed substantially to these investigations. However, these reflectivity techniques are generally limited by the absence of crucial phase information, the relatively small contribution of the amphiphile to the scattering-length density contrast across the interface, and the relatively limited range of momentum transfer available perpendicular to the interface. Although several procedures have been developed to provide model-independent solutions to the phase problem, there remains a limited ability to distinguish features of slightly differing contrast (i.e., the "sensitivity") as well as their minimum allowable separation (i.e., the "spatial resolution") along the length of the scattering-length density profile derived from the reflectivity data via solution to the phase problem. Here, we demonstrate how the well-known interferometric approach can be extended to the structural investigation of otherwise unperturbed Langmuir monolayers of these amphiphiles to provide a direct solution to the phase problem and importantly, substantially enhance both the sensitivity and the spatial resolution in the derived profiles.

DOI: 10.1103/PhysRevE.81.021604 PACS number(s): 68.18.−g, 61.05.cm

I. INTRODUCTION

Langmuir monolayers of organic and bio-organic amphiphilic macromolecules formed at liquid-gas interface provide an important system for the study of the structure and properties of these amphiphiles at the interface between polar and nonpolar environments [1]. These two-dimensional (2D) systems can serve not only as models for the study of complex processes exhibited by biological membranes [2], but also as precursors in the formation of new ultrathin film materials with superior properties [3]. Importantly, these Langmuir monolayers offer the possibility of controlling both the intramolecular structure and intermolecular ordering of the amphiphilic macromolecules via several available adjustable parameters including surface pressure, temperature, relative concentrations of the macromolecular species in mixtures, and the compositions of both the aqueous subphase and the gaseous superphase with respect to the interface [4]. These ordered Langmuir monolayers of amphiphiles can also serve as templates for the directed 2D assembly of components soluble in the subphase at the amphilphile-subphase interface, ranging from atoms to proteins and nanoparticles [5].

These Langmuir monolayers can subsequently be conveniently transferred onto the bare or alkylated surface of solid inorganic substrates using Langmuir-Blodgett (LB) [6] or Langmuir-Schaefer (LS) [7] techniques to prepare ultrathin organic or bio-organic films at the solid-liquid or solid-gas interface. These so-transferred ultrathin films on solid inorganic substrates are more generally used for investigating both their structure and particularly their properties [4]. However, LB and LS depositions are nonequilibrium techniques, and therefore the intramolecular structure and intermolecular ordering of the macromolecular species prepared in the precursor Langmuir monolayer may not necessarily be preserved upon transfer onto the solid substrate surface [8–11]. Hence, it is important to study these structural parameters both prior to and following their transfer onto solid substrates.

In the structural characterization of Langmuir monolayers of organic and bio-organic amphiphiles at the liquid-gas interface, both specular and off-specular x-ray and neutron reflectivity and grazing-incidence x-ray diffraction are proven key techniques [4,6]. However, the specular reflectivity techniques are generally limited by the absence of crucial phase information, the relatively small contribution of the amphiphile (in the absence of heavy-atom or isotopic labeling in the x-ray and neutron cases, respectively) to the scattering-length density contrast across the interface, and the relatively limited range of momentum transfer available perpendicular to the interface. Thus, although several procedures have been developed to provide model-independent solutions to the phase problem (e.g., [12] and references therein), there remains a limited ability to distinguish features of slightly differing contrast along the length of the scattering-length density profile derived from the reflectivity data via solution to the phase problem, thereby defining the "sensitivity" of the technique. In addition, the minimum allowable separation of these features along the length of the scattering-length density profile, defining the "spatial resolution," remains low, e.g., at 10–15 Å level.

In the past, the interferometric approach has been successfully employed in specular x-ray and neutron reflectivity measurements [13,14] of organic and bio-organic monolayers, either transferred onto or self-assembled on the surface of solid inorganic substrates, including monolayers of vecto-

*Corresponding author. jkblasie@sas.upenn.edu

rially oriented designed artificial peptides and natural proteins [15–17]. This approach effectively resolves the limitations to the specular reflectivity techniques described above. In this approach, an inorganic multilayer structure is fabricated on the surface of the solid inorganic substrate to provide the reference structure critical for phasing the reflectivity data. Manipulation of the number, thickness, and scattering-length density of the layers comprising this multilayer reference structure is key to optimizing both the enhanced sensitivity and spatial resolution achievable. However, the proven advantages of this interferometric approach have not yet been applied in the investigation of the structure of Langmuir monolayers of amphiphiles at the liquid-gas interface. The main challenge is the accurate positioning of the internal reference structure precisely parallel to the necessarily horizontal interface, in sufficiently close proximity to the Langmuir monolayer without perturbing the film.

In this article, we describe the development of the interferometric approach for x-ray reflectivity in the structural characterization of Langmuir monolayers, without perturbation of the film at water-helium interface. We have applied this technique to a noncrystalline, densely packed 2D ensemble of a designed amphiphilic 4-helix bundle peptide to demonstrate the substantial enhancement of both the sensitivity and the spatial resolution achievable in nonresonance x-ray reflectivity. This peptide can incorporate complex chromophores containing a transition metal with high specificity. The Langmuir monolayer of the peptide-chromophore complex has a low in-plane density of the resonant transition-metal atom. We utilize this fact to further demonstrate the substantial enhancement of the sensitivity provided by the interferometric approach in resonance x-ray reflectivity. The interferometric approach developed in this work for x-ray reflectivity can be readily extended to neutron reflectivity.

II. EXPERIMENT

The development of the interferometric approach for Langmuir monolayers at the water-helium interface utilized a *de novo* designed amphiphilic 4-helix bundle peptide, designated AP0 [18,19]. At high surface pressures, the bundle orients with its long axis perpendicular to the interface with an extension of ~60 Å and each bundle occupying an area of ~500 $Å^2$ in the plane of the monolayer ensemble. While the average electron density of the helices comprising the bundle is somewhat greater than that of the aqueous subphase, there is little variation along the length of the bundle. It was designed to also bind with high specificity extended conjugated chromophores such as RuPZn, comprised of a Zn-porphyrin linked via an ethynyl bridge to a polypyridyl-Ru, which exhibits a large optical hyperpolarizability [20]. The binding of the chromophore into the core of the bundle is achieved via axial ligation of the zinc atom to a histidine residue positioned at a specific site along the length of the α helix. The long axis of the chromophore is aligned along the axis of the bundle resulting in one zinc (or ruthenium) atom per ~500 $Å^2$ in the plane of the monolayer for a helix-chromophore stoichiometry of 4:1. These transition metals exhibit *K* edge resonance x-ray scattering in the x-ray regime.

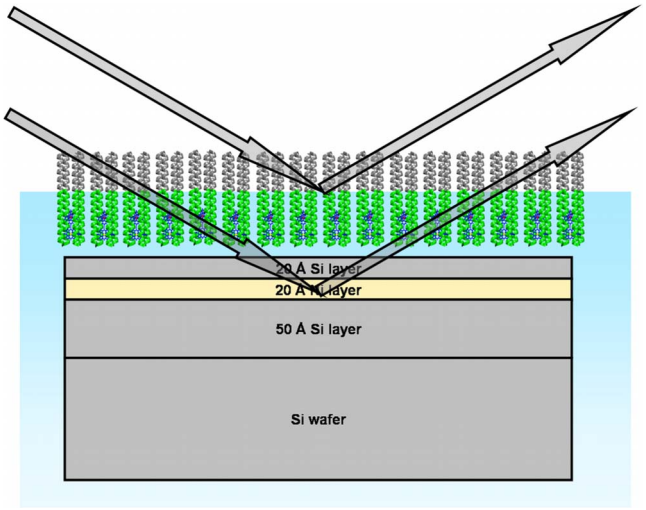

FIG. 1. (Color online) Schematic representation of the interferometric approach to x-ray reflectivity to determine the profile structure of an ultrathin Langmuir film of an amphiphile at the liquid-gas interface. The close proximity of the multilayer reference structure without contacting the otherwise unperturbed Langmuir monolayer of the amphiphile at the liquid-gas interface allows for the critical interference of x rays reflected by the underlying reference structure with those reflected by the amphiphile.

The AP0 peptide itself and the AP0-RuPZn peptide-chromophore complex were spread as monolayers on an aqueous subphase of low ionic strength (1 mM) contained in a Langmuir trough. The procedure employed in the preparation of the spreading solution is described in a previous article [21]. The x-ray reflectivity measurements on these Langmuir monolayers using noninterferometric and interferometric approaches were performed using the liquid surface spectrometer at beamline 9-ID-C of the Advanced Photon Source (APS) at Argonne National Laboratory (ANL), Argonne, IL, USA. The canister enclosing the Langmuir trough was filled with humid He gas in order to reduce the x-ray background scattering arising from air and also to minimize subphase evaporation.

The details of noninterferometric x-ray reflectivity data collection and analysis have been explained in earlier publications [12,18]. Interferometric x-ray reflectivity data collection proceeds in a similar manner once the reference structure is in position. In both the cases, specular x-ray reflectivity is measured in the vertical scattering plane with the out-of-plane angle on the liquid surface spectrometer set to $2\theta_{xy}=0°$, and off-specular background is measured with $2\theta_{xy}=\pm 0.3°$ for half the time on either side of the scattering plane. Later the off-specular background was subtracted from the specular data to obtain the background-corrected data. A schematic diagram of the interferometric approach to x-ray reflectivity is shown in Fig. 1. Initially, the wafer possessing the multilayer reference structure on its upper surface is precisely aligned parallel to the trough and then buried deeply in the subphase. Subsequently, the wafer was slowly raised ultimately coming into juxtaposition with the Langmuir monolayer of the compressed amphiphile at the interface. A separation of 10–100 Å between the monolayer film

and the uppermost surface of the wafer is achieved by the combined use of mechanical and piezoelectric translation. For this purpose, a NTS10 NanoDirect nanopositioner (DTI-NanoTech, Sarasota, FL, USA) was used. Precise control of the separation between the lower surface of the Langmuir monolayer of the amphiphile and the upper surface of the multilayer reference structure is required to retain the structure of the organic/bio-organic ultrathin film at the water-helium interface without perturbation from the proximity of the wafer. With this approach, the incoming x rays are then not only reflected from the Langmuir monolayer of the amphiphile but also from the underlying reference wafer. Hence, the x-ray reflectivity so obtained becomes rich in features due to interference effects between the two reflectivity phenomena. These interference effects are essential to providing a direct solution to the phase problem as well as the substantial enhancement of both the sensitivity and the spatial resolution in the derived electron-density profile across the interface.

The interferometric approach requires the use of an inorganic reference multilayer structure. The optimal reference structure should maximize the interference effects between the multilayer reference structure (which is known from its fabrication specifications and subsequently verified experimentally) and the unknown structure of the Langmuir monolayer of the amphiphile (which is to be determined). These interference effects can be tuned via the fabrication specifications and should ideally range from fully constructive to completely destructive, over the largest possible range of photon momentum transfer perpendicular to the interface, Q_z. Optimization of the parameters of the multilayer reference wafer is dependent on the fabrication method. We found electron-beam evaporation methods to be incapable of producing layers of sufficient uniformity and reproducible minimal thicknesses. Magnetron sputtering was found to provide a more precise control over both the uniformity of the layers and smaller reproducible thicknesses. In addition, the optimization can involve not only the thickness and relative electron densities of the higher and lower contrast layers in the multilayer unit cell but also the number of unit cells in the multilayer superlattice where thickness reproducibility is essential. The number of unit cells should be small, e.g., 1–3, so as to provide phase information continuously over the accessible range of Q_z. In the present work, the fabrication of the multilayer reference structures on silicon wafers was performed at the deposition laboratory of the APS at ANL, Argonne, USA. An optimization procedure, employing a comparison of the simulated specular x-ray reflectivity with that measured from test samples, resulted in the following reference multilayer structure employed in this work, namely, a multilayer comprised of 50 Å Si-20 Å Ni-20 Å Si (henceforth referred as Si-Ni-Si) on a 3″ diameter silicon wafer (n-type Si:P−600-μm-thick, El-Cat Inc., Waldwick, NJ, USA.).

The interferometric analysis of the x-ray reflectivity data was performed in the distorted-wave Born approximation using the computationally efficient, so-called box-refinement algorithm [12,13]. In the noninterferometric analysis of x-ray reflectivity data from a Langmuir monolayer of an amphiphile at the liquid-gas interface, a simple step function, representing the electron-density profile across an ideal interface in the absence of the amphiphile, is used as the input trial structure to initiate the phase refinement. The finite extent of the gradient of the electron-density profile for the Langmuir monolayer at the interface, the powerful "box constraint" determined experimentally from the reflectivity data without phase information, provides the critical constraint for driving the refinement to converge to an acceptable electron-density profile for the monolayer of the amphiphile. However, in the case of the interferometric analysis, x-ray reflectivity with an adjacent reference structure [13,22], the known electron-density profile of the multilayer reference structure is used as the input trial structure to initiate the phase refinement. The fabrication specifications for the multilayer provide initial parameters for its structure which can be refined against the reflectivity from the reference structure itself. The dominance of the reference structure in the phase refinement, due to its greater contrast, results in the box-refinement algorithm converging to the phase solution nearest that for the reference structure, thereby providing directly the electron-density profile of the adjacent organic/bio-organic monolayer.

III. RESULTS AND DISCUSSION

Besides providing a direct solution to the phase problem, the important advantages of using the interferometric approach to x-ray reflectivity measurements include the enhancement of both the sensitivity and the spatial resolution in the structural investigations of Langmuir monolayers of organic/bio-organic amphiphiles at liquid-gas interface. To demonstrate this aspect experimentally, we utilized the AP0-RuPZn peptide-chromophore complex that was spread as Langmuir monolayer at the water-helium interface. A photograph of the experimental setup used for interferometric x-ray reflectivity measurement is shown in Fig. 2. The Si-Ni-Si multilayer reference structure on the surface of a Si wafer was supported at the lower end of a metal rod as shown. Importantly, in order to avoid the penetration of the Langmuir monolayer by the rod supporting the reference structure, an additional stationary barrier was mounted on the Langmuir trough and the metal rod was positioned behind this barrier as shown.

Initially, x-ray reflectivity was first obtained from the Si-Ni-Si reference wafer in helium, but using the same sample chamber as for subsequent measurements of the Langmuir monolayer. For these measurements, the lid of the gas-tight canister enclosing the Langmuir trough was replaced with a lid in two segments, one that could be easily removed, and one with a tilt stage and two vertical translation stages mounted on it. These stages were coupled to a rod passing though a feedthrough in the lid and supporting the reference wafer on its upper surface. The tilt stages allowed the wafer to be precisely aligned in the horizontal plane for the specular x-ray reflectivity measurements from the reference multilayer structure with the upper surface of the wafer positioned higher than the Teflon walls of the Langmuir trough. Then, in order to collect noninterferometric x-ray reflectivity for the Langmuir monolayer of AP0-RuPZn peptide-

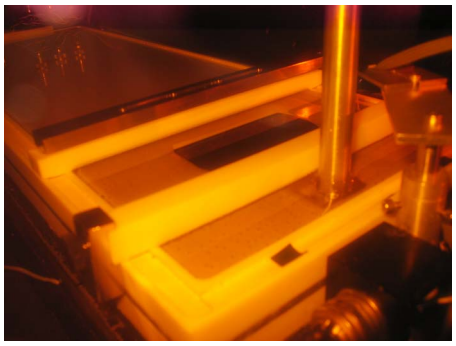

FIG. 2. (Color online) Photograph of the experimental setup used for the interferometric x-ray reflectivity measurements, viewed through the kapton window of the trough canister. The rod supporting the reference structure appears in the foreground separated from the Langmuir monolayer of the AP0-RuPZn amphiphile by the adjacent fixed Teflon barrier. The reference multilayer structure is on the upper surface of the silicon wafer visible in the aqueous subphase on the other side of the fixed barrier. The moving Teflon barrier employed to compress the monolayer of the amphiphile is visible just beyond the reference structure, with a large expanse of only the aqueous subphase behind the moving barrier following compression.

chromophore complex, the Si-Ni-Si reference structure was translated vertically downward by the mechanical vertical translation stage until it was submerged deeply in the trough and then the trough was filled with aqueous subphase. The AP0-RuPZn peptide-chromophore complex was then spread on the water-air interface and compressed to a surface pressure of 39 mN m^{-1}. A schematic representation of AP0-RuPZn peptide-chromophore complex is shown in Fig. 3(a) and a typical pressure-area isotherm for this amphiphile is shown in Fig. 3(b). This relatively high surface pressure remained stable during all subsequent measurements, which is

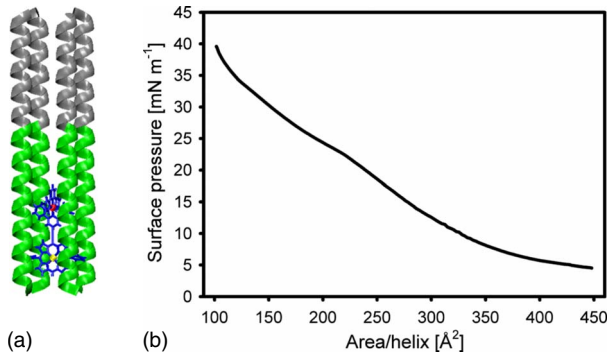

FIG. 3. (Color online) (a) Schematic representation of AP0-RuPZn peptide-chromophore complex. The straight α helices are shown in the ribbon representation, wherein the lower and upper halves representing the hydrophilic and hydrophobic domains, respectively, of the amphiphilic 4-helix bundle AP0. The RuPZn chromophore is shown in the center of the bundle using stick representation, with its zinc and ruthenium atoms shown as dark-colored spheres. (b) A typical pressure-area isotherm for a Langmuir monolayer of the AP0-RuPZn amphiphile. Note the steepness of the isotherm in the higher surface pressure regime, namely, in the vicinity of 39 mN m^{-1} employed in these experiments.

noteworthy considering the steepness of the isotherm in this higher surface pressure regime. The x-ray reflectivity obtained for this compressed monolayer agrees well with the earlier results [21] on the same system, indicating the complete vectorial orientation of the α-helical bundles with their long axis aligned perpendicular to the interface at this surface pressure. For reference, typical Fresnel-normalized specular x-ray reflectivity data for this amphiphile upon compression at three selected surface pressures spanning a large range of the isotherm, corresponding to average area per helix values of 300 $Å^2$, 150 $Å^2$ and 100 $Å^2$, are shown in Fig. 4(a). The corresponding monolayer electron-density profiles, are shown in Fig. 4(b). These profiles demonstrate the nearly continuous orientational transition typical of these amphiphilic 4-helix bundle peptides as described previously [18,19,21], in which the helices are aligned initially parallel to the water-helium interface at lower surface pressures and become progressively oriented more perpendicular to the interface upon compression, with all helices perpendicular to the interface only at the higher surface pressure extreme. Subsequently, the Si-Ni-Si reference wafer was slowly translated vertically upward using the piezoelectric translation until the meniscus over the wafer was seen to rise above the level of the surrounding, unsupported meniscus. Reflectivity collected in this condition showed that the aqueous layer between the wafer and the monolayer, was too thick for any interference effects to be observed (data not shown), and the reflectivity remained essentially the same as it was when the reference wafer was deep in the subphase. At this point, for the first set of multilayer references structures, whose upper surface was hydrophobic (based on macroscopic observations of wetting with aqueous media and estimates of the contact angle), the evaporation of the subphase was intentionally promoted by the rapid flow of *dry* He to facilitate thinning of the intervening water layer between the Langmuir monolayer of the amphiphile and the Si-Ni-Si reference structure. Care was taken not to perturb the Langmuir monolayer at the water-helium interface. When the layer was uniformly thin across the wafer such that the wafer appeared dry but with the meniscus still attached, the reflectivity data exhibited obvious interference effects. Remarkably, the surface pressure remained constant during these operations and during the subsequent reflectivity experiments, measured to an accuracy of ± 1 mN m^{-1}, indicative of the retention of the bundle axis alignment perpendicular to the interface. Thus, we anticipated that the Langmuir monolayer remained undisturbed and that no direct contact was established between the upper surface of the reference structure and the lower surface of monolayer. Once these interference features were observed, a minimal flow of *moist* helium was used to maintain the level of the aqueous subphase and x-ray reflectivity measurements were then performed under these stable interferometric conditions. As described below, the absence of any contact between the upper surface of the reference structure and the lower surface of monolayer was later substantiated in the electron-density profiles derived from the interferometric x-ray reflectivity data that indicated a gap with a thickness of about 10 Å between these two surfaces when the upper surface of the reference structure was hydrophobic.

The Fresnel-normalized x-ray reflectivity data, $R(Q_z)/R_F(Q_z)$, obtained for the Langmuir monolayer of the

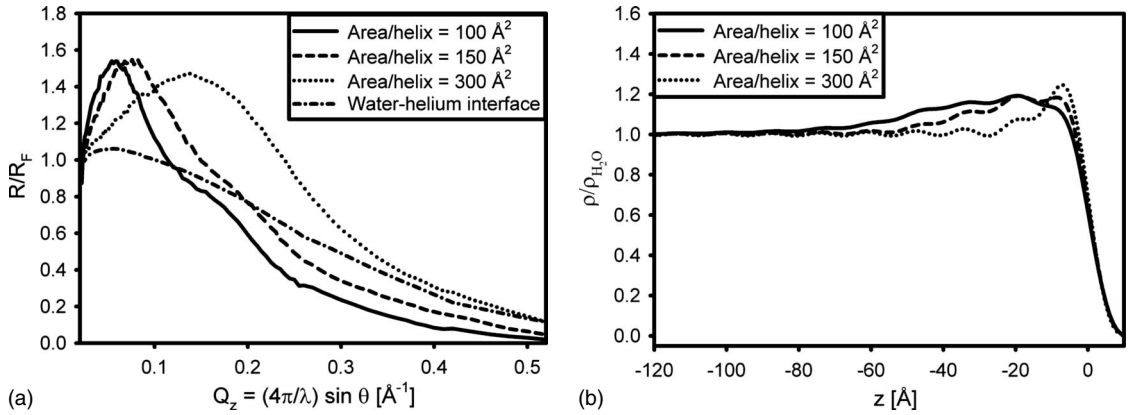

FIG. 4. (a) Fresnel-normalized specular x-ray reflectivity from a Langmuir monolayer of the AP0-RuPZn amphiphile upon compression at three selected surface pressures corresponding to the average area/helix values indicated. Note the expanded ordinate scale compared with that in the subsequent Figs. 5(a) and 6(a). (b) Corresponding monolayer electron-density profiles calculated from the data shown in (a). Note that at the higher surface pressure of 39 mN m^{-1}, corresponding to an average area/helix in the plane of the interface of 100 $Å^2$, the excess electron density arising from the amphiphile at the water-helium interface is relatively uniform over about 50 Å. At this high surface pressure, the bundle axis has become perpendicular to the interface, the helices extending about 60 Å along the profile axis allowing for interfacial roughness at both the peptide-helium interface at $z=0$ Å and the peptide-water interface at $z=-60$ Å. Also note the expanded ordinate scale compared with that in the subsequent Figs. 5(d) and 6(d).

AP0-RuPZn amphiphile employing both the noninterferometric and interferometric approaches are shown in Figs. 5(a) and 5(b), along with the data from the Si-Ni-Si reference structure. A substantial improvement in both the spatial resolution and sensitivity arising from the interference effects is clearly evident from Fig. 5. With regard to the "spatial resolution," note that the signal from the Langmuir monolayer of the amphiphile in the interferometric case is contained in the *difference* between the Fresnel-normalized reflectivity for the reference structure itself and that with the adjacent mono-

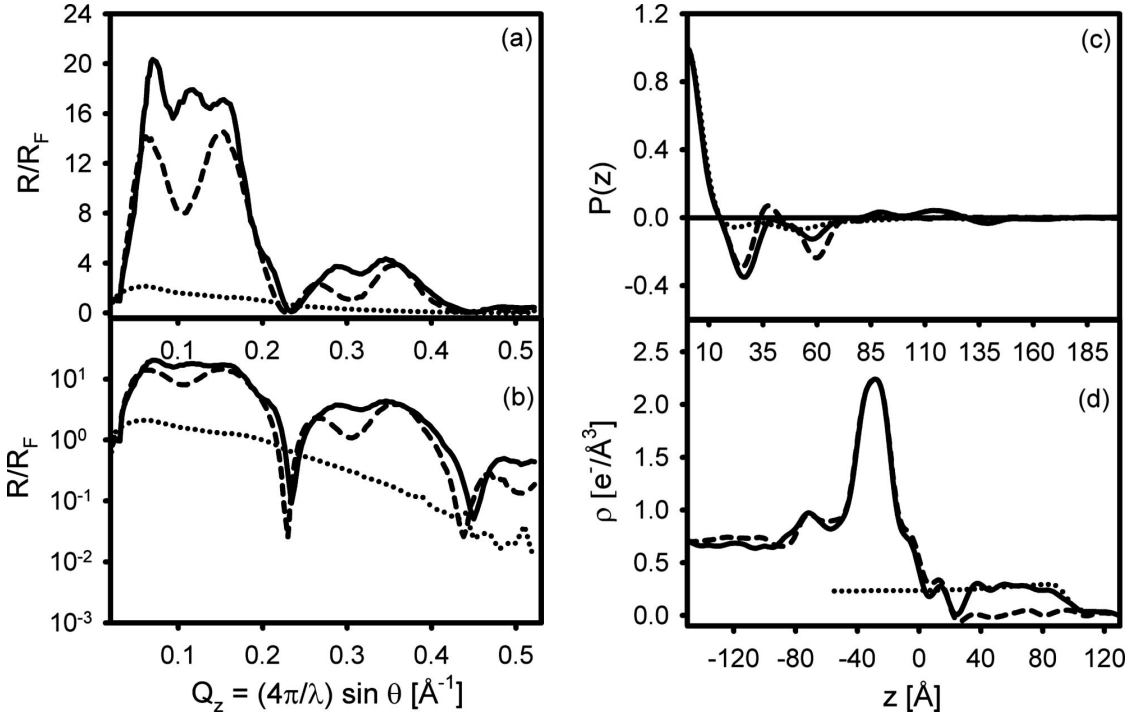

FIG. 5. X-ray reflectivity results (measured at 22 017 eV) from a Langmuir monolayer of the AP0-RuPZn amphiphile obtained using noninterferometric and interferometric approaches shown along with those for the Si-Ni-Si reference structure alone that possessed a macroscopically *hydrophobic* upper surface [dashed lines, Si-Ni-Si reference structure in He; continuous lines, Si-Ni-Si reference structure with adjacent Langmuir monolayer (interferometric case); and dotted lines, Langmuir monolayer of the amphiphile only]. (a) Fresnel-normalized x-ray reflectivity data shown on a linear scale, (b) Fresnel-normalized x-ray reflectivity data shown on a semilogarithmic scale, (c) Patterson (autocorrelation) functions, and (d) electron-density profiles. See text for further description and discussion.

layer of the amphiphile. This relatively large amplitude signal is virtually noiseless, in terms of the counting statistics, extending over the entire range of Q_z investigated, extending apparently, beyond the maximum value of 0.5 $Å^{-1}$, as particularly evident in the semilogarithmic plot in Fig. 5(b). In this case, the *effective* spatial resolution achievable in electron-density profile of the amphiphile derived from these data is simply limited only by the range of momentum transfer investigated. Conversely, for the noninterferometric case, the signal from the Langmuir monolayer of the amphiphile is contained in the features in the Fresnel-normalized reflectivity *that differ significantly* from those in the reflectivity from the clean water-helium interface in the absence of the amphiphile. While these differences are difficult to visualize in Fig. 5 where they appear on the same ordinate scale as for the interferometric case, they are readily apparent on an expanded ordinate scale in Fig. 4(a). These significant features, e.g., maxima and minima, are thereby seen to occur only for $Q_z < 0.25$ $Å^{-1}$, the data becoming as featureless as that of a clean water-helium interface (namely, a simple exponential decay determined by the roughness of the interfaces in the monolayer profile) for larger values of momentum transfer. This severely limits the *effective* spatial resolution in the derived electron-density profile of the amphiphile in the noninterferometric case by at least a factor of two compared to the interferometric case in these experiments, in spite of the fact that data were collected to the same maximum value of Q_z in both cases. Specifically, for the noninterferometric case, features in the electron-density profile separated by less than about 20 Å would not be distinguishable compared with separations of about 10 Å or less for the interferometric case. With regard to "sensitivity," note that the *amplitude* of the signal from the Langmuir monolayer of the amphiphile in the interferometric case, as defined above, is much larger than that for the noninterferometric case over the entire range of Q_z investigated. For example in Fig. 5, this amplitude measured over the regions containing the maxima, where such comparisons remain finite, is already about two to eight times larger for $Q_z < 0.20$ $Å^{-1}$, about 3 to 5 times larger for $0.23 < Q_z < 0.43$ $Å^{-1}$, and about 10 times larger for $0.43 < Q_z < 0.52$ $Å^{-1}$.

Fourier transformation of the Fresnel-normalized data provides the autocorrelation of the gradient of the electron-density profile of the monolayer. This is also known as Patterson function, which determines the maximum extent of the gradient of the electron-density profile across the interface (i.e., the box constraint) because the gradient profile is bounded due to the uniform electron density of the helium superphase above the monolayer and the aqueous subphase below the monolayer. The Patterson functions for the Langmuir monolayer obtained using noninterferometric- and interferometric approaches are shown along with that for the Si-Ni-Si reference structure in Fig. 5(c). In the noninterferometric case, the autocorrelation function exhibits significant features extending only to ~60 Å, in agreement with the expected length of the AP0 peptide (each α-helix of AP0 has 42 residues yielding a length of about 63 considering 1.5 Å per residue along its axis). This indicates that the orientation of the long axis of the 4-helix bundle peptide is perpendicular to the water-helium interface at the higher surface pressure utilized. The Patterson function for the interferometric case has more prominent features extending to larger distances. In particular, these features extend slightly beyond ~150 Å when the monolayer of the amphiphile is adjacent to the reference structure, as compared to only ~90 Å for the reference structure itself.

The electron-density profiles for the Langmuir monolayer of the AP0-RuPZn amphiphile obtained using both the noninterferometric and interferometric approaches are shown, along with that for the Si-Ni-Si reference structure, in Fig. 5(d). The peptide-helium interface is at +110 Å for both the noninterferometric and interferometric cases. In the noninterferometric case, the peptide-water interface is at +50 Å, illustrating that the peptide is ~60 Å in length [more readily evident when shown on an expanded ordinate scale as in Fig. 4(b)]. For the Si-Ni-Si reference structure and for the interferometric case with the adjacent Langmuir monolayer of the amphiphile, the various regions of the profile can be assigned to the following layers:

(i) $-150 < z < -90$ Å: the underlying Si wafer;

(ii) $-90 < z < -80$ Å: native SiO_2 on the wafer surface;

(iii) $-80 < z < -40$ Å: first amorphous Si layer deposited on the native oxide layer;

(iv) $-40 < z < -15$ Å: amorphous Ni layer deposited on the amorphous Si layer;

(v) $-10 < z < 0$ Å: second amorphous Si layer deposited on the Ni layer; and

(vi) $0 < z < +20$ Å: low-density amorphous SiO_x layer.

All the interfaces in these profiles have a width of about 4 Å. With regard to the multilayer reference structure, the profiles reveal that initially, it is reasonably consistent with the fabrication specifications with the addition of the amorphous SiO_x layer that forms on the surfaces of such multilayer substrates fabricated by either sputtering [23] or molecular-beam epitaxy (MBE) [17]. Furthermore, the reference structure does change somewhat upon exposure to the aqueous subphase in the interferometric experiments with regard to the density of the Ni layer. The electron-density profile in the interferometric case clearly shows the presence of the peptide layer for $+30 < z < +90$ Å of relatively uniform electron density slightly greater than that of water, which is absent in the profile of the reference structure itself in helium. An intervening layer of very low electron density is seen to occur between the hydrophobic upper surface of the reference structure and the lower surface of the peptide layer of ~10 Å thickness. The very low density of this layer is consistent with moist helium vapor, and certainly not bulk water. This feature is robust in that artificially increasing its electron density to that of water, all other features remaining unchanged, results in a calculated Fresnel-normalized x-ray reflectivity that differs substantially from the experimental data. This result is consistent with the fact that the surface of this particular multilayer reference structure was found to be quite hydrophobic (see below for the hydrophilic case), based on macroscopic observations of wetting with aqueous media and estimates of the contact angle. Lastly, the low amplitude, minimum wavelength undulations in the electron-density profiles can be ascribed to truncation of the Fourier transform employed in the analysis. Such undulations are the simple manifestation of the Fourier representation of the

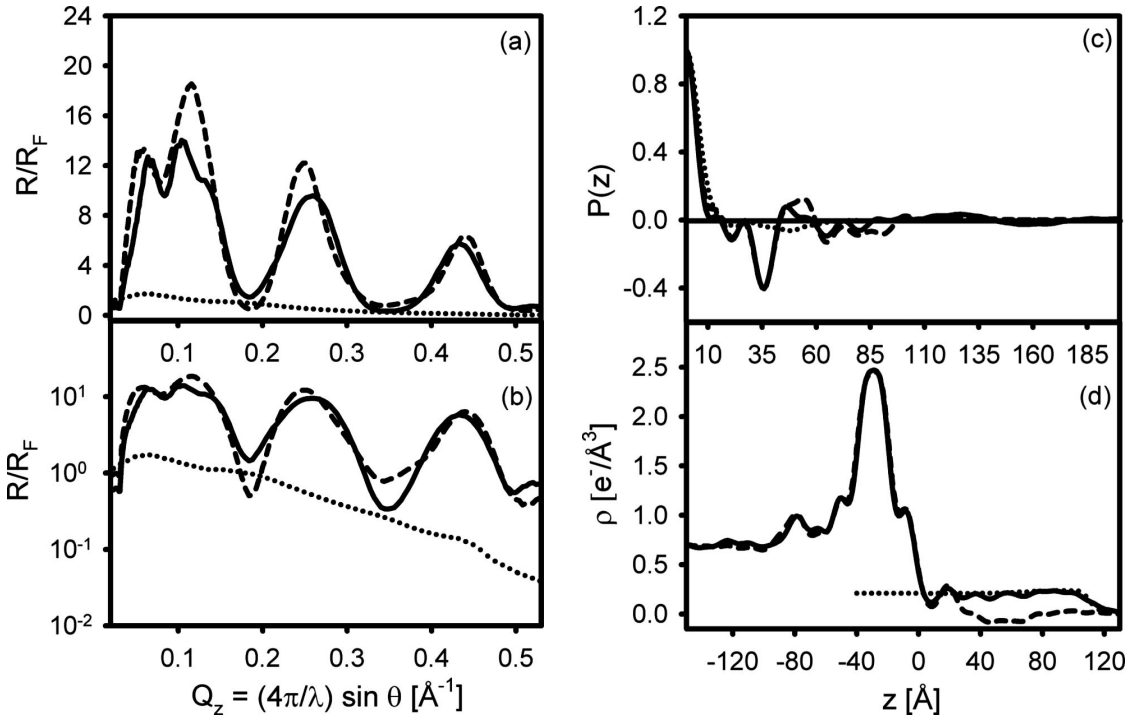

FIG. 6. X-ray reflectivity results (measured at 9559 eV) from a Langmuir monolayer of the AP0-RuPZn amphiphile obtained using noninterferometric and interferometric approaches shown along with those for the Si-Ni-Si reference structure alone that possessed a macroscopically *hydrophilic* upper surface [dashed lines, Si-Ni-Si reference structure in He; continuous lines, Si-Ni-Si reference structure with adjacent Langmuir monolayer (interferometric case); and dotted lines, Langmuir monolayer of the amphiphile only]. (a) Fresnel-normalized x-ray reflectivity data shown on a linear scale, (b) Fresnel-normalized x-ray reflectivity data shown on a semilogarithmic scale, (c) Patterson (autocorrelation) functions, and (d) electron-density profiles. See text for further description and discussion.

one-dimensional (1D) profile and they define the local average electron density within any particular region of the profile. For any two profiles containing such errors to be significantly different, they must satisfy well-defined criteria thoroughly described by Strzalka *et al.* [24]. Such an analysis of electron-density distributions and their differences is typical of crystallographic studies in higher dimensions, e.g., 2D and three-dimensional. Other representations of such 1D profiles obtained via either model refinement or alternative approaches to solving the phase problem manifest such errors differently, as recently described in detail by Valincius *et al.* [25].

Given the macroscopically hydrophobic surface of the multilayer reference structure described above, a second set was fabricated. Although the layers in these were not found to be as uniform as those described above for the first set, as will be described below, the upper surface of these multilayer reference structures was found to be macroscopically hydrophilic, on the same basis, with profound implications. Similar to the previous case, a high rate of *dry* He flow was used to promote thinning of the intervening water layer until the interference features appeared, followed by a return to a minimal flow rate of *moist* helium during the reflectivity measurements under stable interferometric conditions. It is noteworthy to mention that under these measurement conditions (i.e., *moist* helium), the change in the thickness of the intervening water layer due to evaporation was found to be negligible. Repeated subsequent reflectivity scans reproduced very well to within the counting statistics, indicating that the water layer thickness remained constant over a period of about 4 h. The substantial improvement in both the spatial resolution and sensitivity arising from the interference effects is again clearly evident in the Fresnel-normalized reflectivity shown in Figs. 6(a) and 6(b). The effects of the interference phenomena are similarly apparent in the autocorrelation (or Patterson) functions shown in Fig. 6(c). The electron-density profiles for the Langmuir monolayer of the AP0-RuPZn amphiphile obtained using both the noninterferometric and interferometric approaches with this multilayer reference structure are shown, along with that for the Si-Ni-Si reference structure, in Fig. 6(d). While the various layers within the reference structure occur with the regions defined above for the reference structure with the hydrophobic surface, there is more evidence in the electron-density profile of this reference structure for migration of the Ni to the interfaces in the multilayer structure, as evidenced by the maxima at $z \sim -80$, -50, and $+20$ Å. This origin for the latter maximum at $\sim +20$ Å might explain the observed macroscopic hydrophilicity of the upper surface of this reference structure. The second implication of particular significance for these reference structures possessing a hydrophilic upper surface is the fact that the low-density layer intervening between the lower surface of the monolayer of the amphiphile and the hydrophobic upper surface of the reference structure described above has vanished, being replaced with a layer whose electron density is approximately equal that of water, slightly less than that of the amphiphile. Given the similar electron densities of the AP0-RuPZn amphiphile and

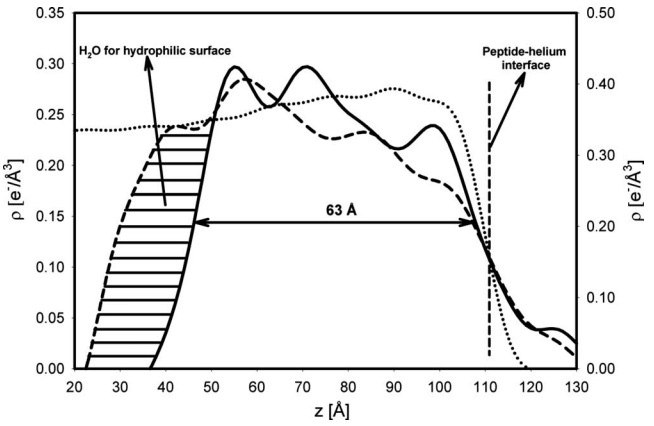

FIG. 7. Difference electron-density profiles for the interferometry case at the water-gas interface, namely, the difference between the electron-density profile for the multilayer substrate with the adjacent Langmuir monolayer of the amphiphile [i.e., continuous lines in Figs. 5(d) and 6(d)] and the profile for the multilayer substrate itself [i.e., dashed lines in Figs. 5(d) and 6(d)]. Here, the continuous-line *difference* profile is for the substrate exhibiting a macroscopically hydrophobic surface, while the dashed-line *difference* profile is for the substrate exhibiting a hydrophilic surface. The intervening water layer on the proximal side (with respect to the multilayer substrate) of the Langmuir monolayer of the AP0-RuPZn amphiphile for the latter hydrophilic surface is shown with cross-hatching. For both these continuous- and dashed-line *difference* profiles, refer to the ordinate scale on the left. The electron-density profile (dotted-line) for noninterferometry case, namely, the electron-density profile of the amphiphile at the water-gas interface at comparable surface pressure [i.e., the continuous-line profile from Fig. 4(b)] is presented for reference. For this dotted-line profile, refer to the ordinate scale on the right. The left-side and right-side ordinate scales are different in order to superimpose the intervening water layer electron density for the interferometric case with the hydrophilic substrate surface and that of the bulk water subphase for the noninterferometric case. See results and discussion section for further details. All three electron-density profiles have been aligned along the profile z axis to make their respective peptide-helium interfaces coincide.

water, the thickness of this intervening water layer can be readily inferred. The ~60 Å length of the amphiphile extending from the monolayer-helium interface at ~+120 Å, places the lower surface of the amphiphile at ~+60 Å. With the upper surface of the reference structure at ~+25 Å, this intervening water layer would be ~35 Å thick. The results described above suggest that macroscopic polarity of the upper surface of the multilayer reference should be intentionally controlled. This can be accomplished via suitable alkylation [26].

A substantial enhancement of both the sensitivity and spatial resolution achievable in *nonresonance* specular x-ray reflectivity employing the interferometric approach is more evident from a closer examination of the electron-density profiles for the amphiphile shown in Figs. 5(d) and 6(d), compared with that for the noninterferometric case from Fig. 4 at comparable surface pressures. For the interferometric case, the *difference* electron-density profile shown in Fig. 7 for the multilayer substrate exhibiting a macroscopically *hydrophobic* surface (continuous-line profile) is that of the amphiphile itself, hydrated with water-saturated helium at either surface (i.e., proximal and distal with respect to the substrate surface). This situation results in the maximum electron density contrast for the amphiphile at both the proximal and distal ends of the amphiphilic 4-helix bundle peptide within the Langmuir monolayer. The peptide-gas interfaces are seen to be relatively well defined (i.e., relatively "narrow"), the electron density of the amphiphile is relatively uniform over its entire length, and the width (full width at half maximum) of the amphiphile's profile structure is 63 Å, precisely that expected for an α-helix comprised of 42 residues oriented perpendicular to the plane of the monolayer. Overall, this profile structure of the amphiphile within the Langmuir monolayer exhibits a relatively "square" shape. The *difference* electron-density profile shown in Fig. 7 for the multilayer substrate exhibiting a macroscopically *hydrophilic* surface (dashed-line profile) is that of the amphiphile itself with the intervening layer of water on the proximal side of the monolayer. The peptide-water interface at the proximal end of the bundle remains apparent, although the profile of the amphiphile itself is somewhat less uniform over its length, likely due to a greater incorporation of the RuPZn chromophore within the hydrophilic domain forming the proximal end of the bundle for this particular monolayer [27]. By comparison, the features described above for the profile of the amphiphile itself in the interferometric case are not so apparent for the noninterferometric case (dotted-line profile) from Fig. 7. For example, the peptide-helium and peptide-water interfaces are much less well defined (i.e., more "broad"), especially the latter, making a determination of the length of the bundle perpendicular to the interface problematic. Worse, the excessive breadth of the latter interface could, in principle, arise from the undesirable unwinding of the α helices at the end of the bundle's hydrophilic domain. Lastly, the electron density of the amphiphile over its length has much less uniform "more rounded" shape, more like that of a single broad maximum. These several "deficiencies" noted for the noninterferometric case are seen, via this detailed comparison, to arise from the limited "effective" spatial resolution achievable with normal reflectivity, described earlier in this section, in the absence of the key interference effect provided by this interferometric approach.

Although a substantial enhancement of both the sensitivity and spatial resolution achievable in *nonresonance* specular x-ray reflectivity employing the interferometric approach has been clearly demonstrated by the results described above, the enhancement of the sensitivity aspect is particularly evident in *resonance* specular x-ray reflectivity with interferometry. Previously, we have investigated the utility of resonance specular x-ray reflectivity without interferometry, using Langmuir monolayers of a simple organic amphiphile, 2-bromo stearic acid [29]. Strong resonance effects with excellent signal-to-noise ratio were observed about the Br K-edge, where the in-plane density of the resonant Br atom was relatively high at ~25 $Å^2$ per Br atom following compression of the monolayer. Subsequently, we attempted to utilize the same resonance x-ray reflectivity approach to localize the Zn atom and the Ru atom of the RuPZn chromophore along the length of the amphiphilic 4-helix bundle

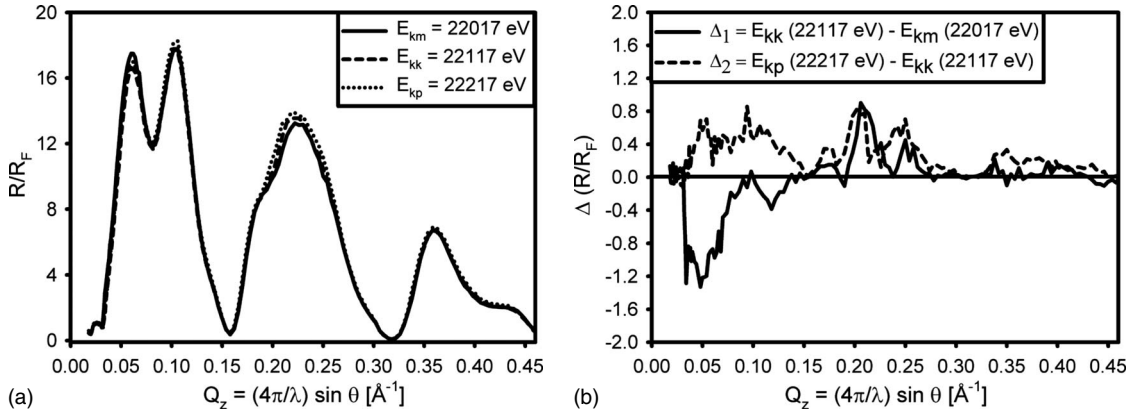

FIG. 8. Resonance specular x-ray reflectivity from a Langmuir monolayer of the AP0-RuPZn amphiphile about the Ru *K* absorption edge obtained using the interferometric approach described in this work. (a) Fresnel-normalized reflectivity at the three x-ray energies, namely, the edge energy of 22 117 eV and 22 117 eV $\pm$ 100 eV. Energy-dependent resonance effects are apparent. These are more apparent in the differences shown in (b).

AP0-RuPZn employed in this work. As noted earlier, the in-plane density of the resonant Zn and Ru atoms following compression of a Langmuir monolayer of this amphiphile to orient the bundle axis perpendicular to the water-helium interface is over an order of magnitude lower at $\sim$500 Å^2 per Zn or Ru atom. As a result, resonant effects about the Zn and Ru *K* edges were not observable. With interferometric enhancement, we have now observed significant resonance effects from the AP0-RuPZn complex about the Ru *K* edge at 22 117 eV. The results are shown in Fig. 8. In these experiments, a factor derived from the energy dependence of the specular x-ray reflectivity from the water-helium interface was used to correct the data for systematic effects, analogous to the procedure used in [29]. Furthermore, a standard signal-averaging procedure was utilized involving a cyclic variation of the x-ray energy about the *K* edge, namely, *K*-Δ, *K*, *K* +Δ, *K*, etc., where Δ=100 eV, to identify and separate any changes in the specular x-ray reflectivity arising simply from evolution of the specimen during data collection (likely due to radiation damage) from the true resonance effects. The Fresnel-normalized specular x-ray reflectivity data shown in the Fig. 8 for each of the three energies about the *K* edge investigated are the average over two cycles. The analysis of these resonance data will be reported separately.

IV. CONCLUSIONS

Langmuir monolayers provide an important system for the investigation of the intramolecular structure and intermolecular ordering of organic and bio-organic macromolecular amphiphiles at an interface between polar and nonpolar media, e.g., the liquid-gas interface. Specular x-ray and neutron reflectivity have contributed substantially to these investigations. We have demonstrated how the well-known interferometric approach can be extended to the structural investigation of otherwise unperturbed Langmuir monolayers of these amphiphiles to provide not only a direct solution to the phase problem, but also and importantly, a substantial enhancement in both the sensitivity and the spatial resolution achievable in the derived profiles. The enhancement in sensitivity can be especially important in resonance x-ray reflectivity experiments where the in-plane density of resonant atoms in the plane of the monolayer is low.

ACKNOWLEDGMENTS

This work was supported primarily by a grant from Department of Energy Biomolecular Materials Program No. DE-FG02-04ER46156 (V.K. and J.K.B.). Partial support was provided by National Science Foundation NSEC Program No. DMR-0425780 (J.S.). We thank W. Pennie for fabricating the stationary barrier and wafer holders used for the experiments. Use of the Advanced Photon Source was supported by the U.S. Department of Energy, Office of Science, Office of Basic Energy Sciences, under Contract No. DE-AC02-06CH11357.

[1] G. L. Gaines, *Insoluble Monolayers at Liquid-Gas Interface* (Interscience, New York, 1966).

[2] J. A. Zasadzinski, J. Ding, H. E. Warriner, F. Bringezu, and A. Waring, Curr. Opin. Colloid Interface Sci. **6**, 506 (2001).

[3] M. Clemente-Leon, C. Mingotaud, C. J. Gomez-Gracia, E. Coronado, and P. Delhaes, Thin Solid Films **327-329**, 439 (1998).

[4] G. Roberts, *Langmuir-Blodgett Films* (Plenum, New York, 1990).

[5] S. Acharya, J. P. Hill, and K. Ariga, Adv. Mater. **21**, 2959 (2009).

[6] A. Ulman, *Ultrathin Organic Films* (Academic, San Diego, 1991).

[7] C. Nicolini, *Molecular Bioelectronics* (World Scientific, Sin-

gapore, 1996).
[8] M. Engel, H. J. Merle, I. R. Peterson, H. Riegler, and R. Steitz, Ber. Bunsenges. Phys. Chem **95**, 1514 (1991).
[9] M. C. Shih, J. B. Peng, K. G. Huang, and P. Dutta, Langmuir **9**, 776 (1993).
[10] V. Brzezinski and I. R. Peterson, J. Phys. Chem. **99**, 12545 (1995).
[11] V. M. Kaganer, H. Moehwald, and P. Dutta, Rev. Mod. Phys. **71**, 779 (1999).
[12] J. K. Blasie, S. Zheng, and J. Strzalka, Phys. Rev. B **67**, 224201 (2003).
[13] A. M. Edwards, J. A. Chupa, R. M. Strongin, A. B. Smith III, J. K. Blasie, and J. C. Bean, Langmuir **13**, 1634 (1997).
[14] L. R. Kneller, A. M. Edwards, C. E. Nordgren, J. K. Blasie, N. F. Berk, S. Krueger, and C. F. Majkrzak, Biophys. J. **80**, 2248 (2001).
[15] S. Xu, M. A. Murphy, S. M. Amador, and J. K. Blasie, J. Phys. I **1**, 1131 (1991).
[16] J. Strzalka, X. Chen, C. Moser, P. L. Dutton, J. C. Bean, and J. K. Blasie, Langmuir **17**, 1193 (2001).
[17] J. A. Chupa, J. P. McCauley, R. M. Strongin, A. B. Smith III, J. K. Blasie, L. J. Peticolas, and J. C. Bean, Biophys. J. **67**, 336 (1994).
[18] S. Ye, J. Strzalka, B. M. Discher, D. Noy, S. Zheng, P. L. Dutton, and J. K. Blasie, Langmuir **20**, 5897 (2004).
[19] S. Ye, B. M. Discher, J. Strzalka, T. Xu, S. P. Wu, D. Noy, I. Kuzmenko, T. Gog, M. J. Therien, P. L. Dutton, and J. K. Blasie, Nano Lett. **5**, 1658 (2005).
[20] T. G. Zhang, Y. X. Zhao, I. Asselberghs, A. Persoons, K. Clays, and M. J. Therien, J. Am. Chem. Soc. **127**, 9710 (2005).
[21] J. Strzalka, T. Xu, A. Tronin, S. P. Wu, I. Miloradovic, I. Kuzmenko, T. Gog, M. J. Therien, and J. K. Blasie, Nano Lett. **6**, 2395 (2006).
[22] M. A. Murphy, J. K. Blasie, L. J. Peticolas, and J. C. Bean, Langmuir **9**, 1134 (1993).
[23] S. Xu, R. F. Fischetti, J. K. Blasie, L. J. Peticolas, and J. C. Bean, J. Phys. Chem. **97**, 1961 (1993).
[24] J. Strzalka, J. Liu, A. Tronin, I. Y. Churbanova, J. S. Johansson, and J. K. Blasie, Biophys. J. **96**, 4164 (2009).
[25] G. Valincius, Frank Heinrich, R. Budvytyte, D. J. Vanderah, D. J. McGillivray, Y. Sokolov, J. E. Hall, and M. Loesche, Biophys. J. **95**, 4845 (2008).
[26] A. M. Edwards, K. Zhang, C. E. Nordgren, and J. K. Blasie, Biophys. J. **79**, 3105 (2000).
[27] The compression ratio for the Langmuir trough employed in these experiments did not permit the implementation of both (a) the interferometric approach and (b) the *in situ* measurement of the chromophore content in the Langmuir monolayer of AP0-RuPZn amphiphile, with the latter employing a portable multipass UV-vis spectrophotometer [28]. As a result of such measurements, we know that spreading the AP0-RuPZn amphiphile from detergent solution at the water-gas interface, as described in the experimental section, can result in a substantial variation in the chromophore in-plane density in the monolayer, the area per chromophore varying by as much as 150–250 $Å^2$. A new trough has been recently constructed to alleviate this problem.
[28] A. Tronin, J. Strzalka, V. Krishnan, H. C. Fry, M. J. Therien, I. Kuzmenko, and J. K. Blasie, Rev. Sci. Instrum. **80**, 033102 (2009).
[29] J. Strzalka, E. DiMasi, I. Kuzmenko, T. Gog, and J. K. Blasie, Phys. Rev. E **70**, 051603 (2004).